JOURNAL OF MATERIALS SCIENCE 25 (1990) 5077–5080

# Determination of $K_{ISCC}$ by indentation in ceramics

K. M. LIANG
*Tsinghau University, Beijing, People's Republic of China*
R. TORRECILLAS, G. ORANGE, G. FANTOZZI
*GEMPPM (CRRACS), Bâtiment 502, INSA de Lyon, 69621 Villeurbanne, France*

A new method is presented for the determination of resistance to crack propagation of stressed ceramics in corrosive environments.

## 1. Introduction

A decrease in strength with time under load is often observed for many structural ceramics and glasses used in ambient environments. This phenomenon, commonly referred to as SCC (stress corrosion cracking), static fatigue or delayed failure, results, at least in part, from slow growth of preexisting flaws in the materials. The small flaws grown until they are large enough to result in catastrophic failure. Therefore, investigating the resistance of materials to stress corrosion cracking and finding a simple way to measure $K_{ISCC}$ (the threshold stress intensity factor in a certain environment) are very important.

Generally, some methods (e.g. DT, DCB and SENB) are used to measure $K_{ISCC}$ for metallic materials in corrosive conditions. These methods are, however, difficult to be used for ceramics. Recently, indentation techniques are considered as a simple method to measure the critical stress intensity factor ($K_{IC}$) for brittle materials [1–5]. We report herein the application of indentation techniques for determining the $K_{ISCC}$ of ceramics.

## 2. Theory

### 2.1. Analysis of stress by indentation

The advent of indentation fracture mechanics [1] has provided a fundamental basis for analysing the apparently complex deformation–fracture response of ceramics to controlled sharp-contact events. Evans and Charles [2], Lawn *et al.* [3] and Anstis *et al.* [4] analysed the stress field produced by indentation. Lawn *et al.* [3] established a model in which the complex elastic–plastic field beneath the indenter is resolved into elastic and residual components. Anstis *et al.* [4] analysed the contribution of elastic and residual components to the radial cracks. At the indentation surface, the elastic component is compressive and the residual component is tensile. The elastic component is reversible and the residual component is irreversible. Hence when the indenter is unloaded (Fig. 1), while the elastic field is removed, the residual component remains. The residual component is, therefore, considered as the driving force responsible for expanding the crack system into its ultimate configuration. In this case the indentation cracks are stressed by the plastic zone. At the crack tip, the stress intensity factor ($K_I$) is correspondent with the residual force ($P_r$) and is a function of the crack length ($c$)

$$K_I = f(c, P_r) \quad (1)$$

Since, the residual force is a function of applied load ($P$) for the indenter

$$P_r = f(P) \quad (2)$$

therefore

$$K_I = f(c, P) \quad (3)$$

Lawn *et al.* [3] and Anstis *et al.* [4] supposed that the crack system was subject to conditions of mechanical equilibrium both during and after the contact event, such that the radial cracks remain stable at $K_I = K_{IC}$. Liang, Orange and Fantozzi [5] obtained an universal formula to calculate $K_{IC}$ for any brittle material and for any load applied by the Vickers indenter

$$14\left(\frac{K_{IC}\phi}{Ha^{1/2}}\right)\left(\frac{H}{E\phi}\right)^{0.4}\left[1 - 8\left(\frac{4\nu - 0.5}{1 + \nu}\right)^4\right] = \left(\frac{c}{a}\right)^{(c/18a)-1.51} \quad (4)$$

where $E$ is the Young's modulus, $\nu$ the Poisson's ratio, $H$ the hardness, $a$ the half diagonal of the Vickers indent, $c$ the radius of the surface crack and $\phi$ a constraint factor ($\approx 3$).

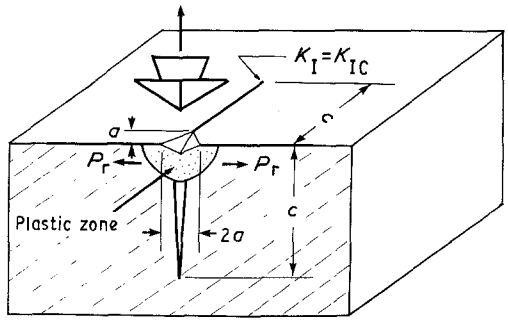


*Figure 1* Residual stress component as the driving force for cracking at complete unload.

0022–2461/90 $03.00 + .12 

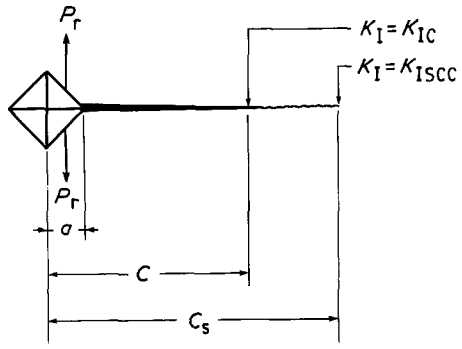


*Figure 2* Indentation cracks propagate in corrosive environments.

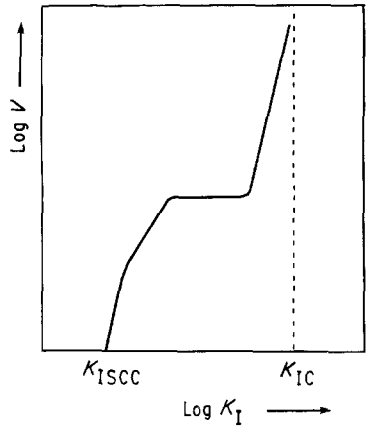


*Figure 3* Velocity of crack propagation plotted against the stress intensity factor at the crack tip.

## 2.2. Stress corrosion cracking

When a piece of material containing indentation cracks is immersed in a corrosive environment, the cracks will propagate because of the existence of the residual component and of the corrosive medium. The length of crack would increase from $c$ to $c_s$ and the stress intensity factor ($K_I$) of the crack tip would decrease to $K_{ISCC}$ (Fig. 2). The velocity (Fig. 3) of crack propagation is given by

$$V = AK_I^n \tag{5}$$

where $A$ and $n$ are constants for a particular material and a given set of test conditions.

When $K_I$ attains the value of the threshold stress intensity factor ($K_{ISCC}$), the crack stops propagating. $K_{ISCC}$ is a property of material and it has the same importance as $K_{IC}$. The value of $K_{ISCC}$ depends upon the material and upon the corrosive conditions. For certain environments, we must, therefore, choose the materials which have sufficiently large values of $K_{ISCC}$. For the measurement of $K_{ISCC}$, we propose to use $c_s$ and $K_{ISCC}$ instead of $c$ and $K_{IC}$ in Equation 4

$$14\left(\frac{K_{ISCC}\phi}{Ha^{1/2}}\right)\left(\frac{H}{E\phi}\right)^{0.4}\left[1 - 8\left(\frac{4\nu - 0.5}{1 + \nu}\right)^4\right] = \left(\frac{c_s}{a}\right)^{(c_s/18a)-1.51} \tag{6}$$

## 3. Experimental procedure

The materials chosen for our study and their mechanical properties are presented in Table I. The surfaces of specimens were polished successively with 6, 1 and 0.1 $\mu$m diamond pastes before being subjected to measurement.

Fracture toughness ($K_{IC}$) was determined by SENB and by Indentation techniques. For SENB technique, the specimens were notched with a low speed diamond saw to a relative depth ($a/W$) $\approx$ 0.4 and their notch radius was set at about 40 $\mu$m. They were subjected to the four-point flexion mode test at room temperature (speed of displacement = 0.1 mm min$^{-1}$). For indentation measurements the specimens were indented on the polished surface with a Vickers tester using loads ranging from 1 to 100 N. The values of $c$ and $a$ were measured by a microscope and the value of $K_{IC}$ was calculated using equation 4.

After indentation, the specimens were immersed in water containing 4 wt % NaCl at room temperature. After 200 h, all the cracks stopped propagating, then, the crack lengths ($c_s$) were measured and equation 6 was used to calculate $K_{ISCC}$.

Finally, the specimens were broken from the indented points by bending for examining the fractured and indented surfaces as well as crack profiles by scanning electron microscope (SEM).

## 4. Results and discussion

### 4.1. Indentation studies under applied loads and $K_{ISCC}$ results

Fig. 4 shows that for a certain material, the value of $K_{ISCC}$ is independent of loads applied by indentation. This phenomenon indicates that the indentation cracks stop propagating when $K_I$ of the crack tips attains $K_{ISCC}$ and that Equation 6 is a useful formula to evaluate $K_{ISCC}$.

Indentation method can, therefore, not only be used to determine $K_{IC}$, but also to determine $K_{ISCC}$. The values of $K_{IC}$ and $K_{ISCC}$ obtained are presented in Table II for the materials listed in Table I.

TABLE I Mechanical properties of materials

| Material | $E$ (GPa) | $H$ (GPa) | $\nu$ | $K_{IC}$ (MPa m$^{1/2}$) | |
|---|---|---|---|---|---|
| | | | | SENB | Indentation |
| Yttria | 167 | 8.1 | 0.298 | – | 3.0 |
| Mullite | 204 | 12.0 | 0.200 | 2.0 | 2.0 |
| ZAM 10 (75 Mullite-25$ZrO_2$) | 205 | 11.8 | 0.250 | 3.6 | 3.6 |
| ZAM 11 (56 Mullite-18$ZrO_2$-26$Al_2O_3$) | 224 | 12.2 | 0.250 | 4.5 | 4.6 |
| ZAM 12 (11 Mullite-17$ZrO_2$-72$Al_2O_3$) | 297 | 12.3 | 0.270 | 5.0 | 5.5 |

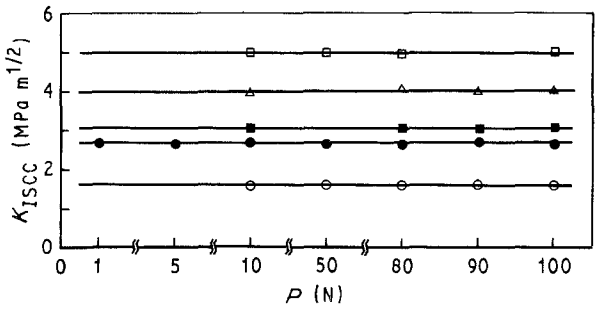


*Figure 4* Values of $K_{ISCC}$ measured by indentation using different loads for different materials (● yttria, ○ mullite, ■ ZAM 10, △ ZAM 11, □ ZAM 12).

## 4.2. Cracks and microstructure

Fig. 2 shows the change of the crack curvature in the surface of a certain material. Under stress corrosion conditions, the crack propogation is controlled by the stress intensity factor and by the effect of corrosion. The value of $K_I$ at the crack tip decreases with the increment of crack, but the effect of corrosion increases. In this case the corrosion takes place more easily at the grain boundary that inside the grain, therefore, the crack curvature is changed.

Fig. 5 shows the profile of crack of yttria which is in correspondence with that of Fig. 2. As shown in Fig. 5, the fractograph can be divided into three zones: (I) indentation cracking zone; (II) stress corrosion cracking zone; and (III) rapid cracking zone which was formed by bending at the indented point. In zones I and III the applied $K_I$ is equal to $K_{IC}$ and the fracture mode is transgranular (Fig. 6a). In zone II the applied $K_I$ is between $K_{IC}$ and $K_{ISCC}$ and the fracture mode

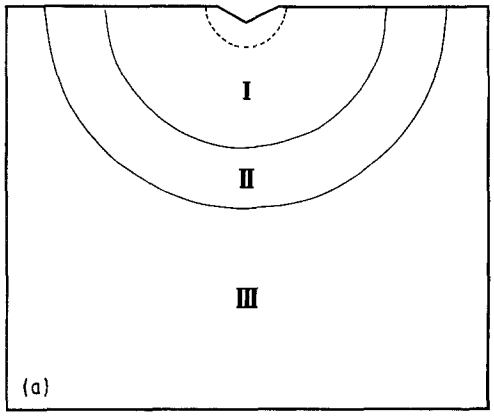


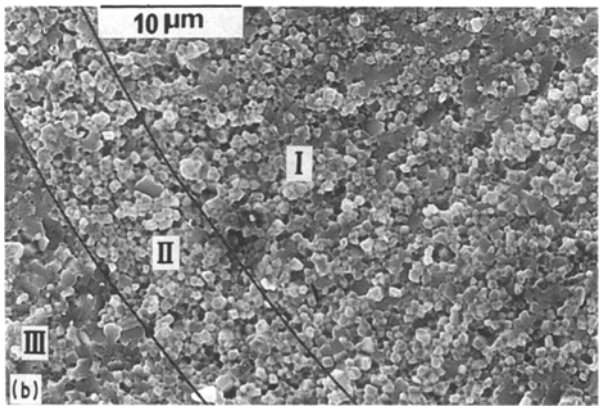


*Figure 5* Fractograph formed in yttria: (I) by indentation; (II) by stress corrosion cracking; (III) by bending.

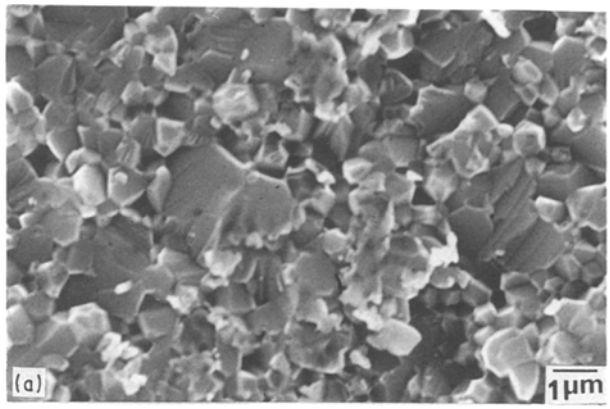


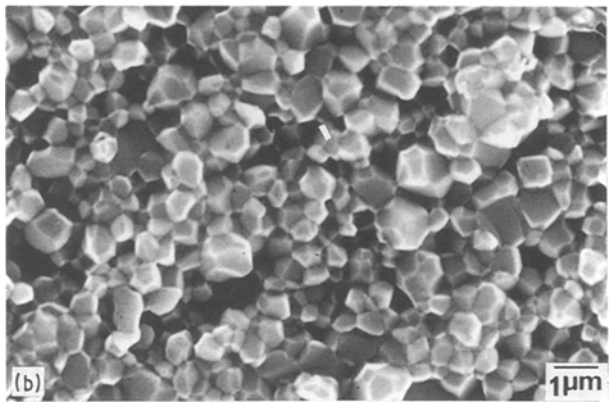


*Figure 6* Fractograph of yttria: (a) intragranular (b) intergranular and transgranular.

is transformed from transgranular to intergranular (Fig. 6b).

This phenomenon can be further explained as follows.

(i) In the absence of stress, the material is attacked completely by the corrosive medium. Charles, Hillig and Wiederhorn [7, 8] explained the rupture of atomic liaisons of glass when it reacts with water under stresses as shown below

$$H\text{–}O\text{–}H + \text{–}Si\text{–}O\text{–}Si\text{–} \rightarrow \text{–}Si\text{–}OH\ HO\text{–}Si\text{–}$$

Fig. 7 shows the cracking model. Yttria could also react with water in a manner similar to glass. At the grain boundary, the atoms are in an unstable state and they could react more easily with a corrosive media than those inside the grains. The crack propagation thus occurs at grain boundaries and the fracture surface appears to be intergranular.

(ii) At high stress, in contrast, the crack propagation is controlled by stresses and the fracture surface appears to be transgranular for yttria (Fig. 6a).

(iii) In the case of stress corrosion cracking, with the diminution of the effect of stress and the increasing of

TABLE II Comparison of the values of $K_{ISCC}$ and $K_{IC}$

| Material | $K_{ISCC}$ (MPa m$^{1/2}$) | $K_{IC}$ (MPa m$^{1/2}$) | $\Delta K_{IC} = K_{IC}-K_{ISCC}$ | $\Delta K_{IC}/K_{IC}$ (%) |
|---|---|---|---|---|
| Yttria | 2.7 | 3.0 | 0.3 | 10 |
| Mullite | 1.6 | 2.0 | 0.4 | 20 |
| ZAM 10 | 3.1 | 3.6 | 0.5 | 14 |
| ZAM 11 | 4.0 | 4.5 | 0.5 | 11 |
| ZAM 12 | 5.1 | 5.5 | 0.4 | 7 |

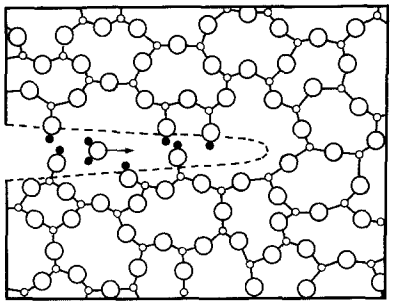

*Figure 7* Model of stress corrosion cracking of glass in water [7, 8].

the influence of corrosion, the fracture feature is transformed from transgranular to intergranular. The stress corrosion region has both intergranular and transgranular features (Fig. 6b).

## 5. Conclusions

The conclusions are as follows

(1) Indentation method can be used to determine the resistance of materials to stress corrosion.

(2) A new formulae is presented to evaluate the value of $K_{ISCC}$ of a material.

## References


1. B. R. LAWN and T. R. WILSHAW, *J. Mater. Sci.* **10** (1975) 1049.
2. A. G. EVANS and E. A. CHARLES, *J. Amer. Ceram. Soc.* **59** (1976) 371.
3. B. R. LAWN, A. G. EVANS and D. B. MARSHALL, *ibid.* **63** (1980) 574.
4. G. R. ANSTIS, P. CHANTIKUL, B. R. LAWN and D. B. MARSHALL, *ibid.* **64** (1981) 533.
5. K. M. LIANG, G. ORANGE and G. FANTOZZI, *J. Mater. Sci.* **25** (1990) 207.
6. T. SATO and M. SHIMADA, *J. Amer. Ceram. Soc.* **68** (1985) 356.
7. R. J. CHARLES and W. B. HILLIG, in Symposium Mechanical Strength and Ways of Improving It (Florence, USCV, 1962) p. 25.
8. S. M. WIEDERHORN, *J. Amer. Ceram. Soc.* **56** (1973) 192.



*Received 10 July*
*and accepted 12 December 1989*